

# Quantum-limited metrology in the presence of collisional dephasing

Y. C. Liu and G. R. Jin\*

*Department of Physics, Beijing Jiaotong University, Beijing 100044, China*

L. You

*Department of Physics, Tsinghua University, Beijing 100084, China*

(Dated: November 16, 2010)

Including collisional decoherence explicitly, phase sensitivity for estimating effective scattering strength  $\chi$  of a two-component Bose-Einstein condensate is derived analytically. With a measurement of spin operator  $\hat{J}_x$ , we find that the optimal sensitivity depends on initial coherent spin state. It degrades by a factor of  $(2\gamma)^{1/3}$  below super-Heisenberg limit  $\propto 1/N^{3/2}$  for particle number  $N$  and the dephasing rate  $1 \ll \gamma < N^{3/4}$ . With a  $\hat{J}_y$  measurement, our analytical results confirm that the phase  $\phi = \chi t \sim 0$  can be detected at the limit even in the presence of the dephasing.

PACS numbers: 03.75.Dg, 03.75.Mn, 03.75.Gg

Parameter estimation with its precision beyond standard quantum limit (SQL) is a long-standing challenge in quantum metrology. The achievable precision depends on the input state [1–7], the observable being measured at output ports [8–10], and the coupling nature of the system Hamiltonian [11–15]. In standard Ramsey interferometry, for instance, resonant atomic frequency  $\chi$  is estimated with a coherent spin state (CSS) that evolves freely under a linear coupling  $\chi\hat{J}_z$ . It has been shown that the precision scales as  $1/N^{1/2}$  (i.e., the SQL) for  $\hat{J}_x$  or  $\hat{J}_y$  measurement [13]. The phase sensitivity can be improved to the so-called Heisenberg limit  $1/N$  with an entangled input state [5–8]. Here, collective spin operators  $\hat{J}_v = \frac{1}{2} \sum_k \hat{\sigma}_v^{(k)}$  with the Pauli matrices  $\hat{\sigma}_{v=x,y,z}$ .

Recently, atom interferometry with Bose-Einstein condensates (BEC) becomes a topical area of study due to potential applications in quantum metrology [7] and quantum information [16]. Elastic collision of condensed atoms can be described by the ‘one-axis twisting’ Hamiltonian  $\chi\hat{J}_z^2$  [17], capable of creating multipartite entanglement and spin squeezing [16–20]. Control of spin dynamics requires precise measurement of the effective interaction strength  $\chi$  [21]. Rey *et al.* [12] recently claimed that even with an initially CSS, the Heisenberg limit is achievable if the free evolution under  $\chi\hat{J}_z$  is simply replaced by  $\chi\hat{J}_z^2$ . A better scaling  $\propto 1/N^{3/2}$  is proposed for the CSS prepared by a  $\pi/4$  or  $3\pi/4$  pulse [13, 14]. Such a super-Heisenberg scaling can also reach in nonlinear optical and nano-mechanical systems [11, 15].

In this brief report, we investigate carefully the effects of collisional dephasing on the BEC-based quantum metrology [12–14], described by the Hamiltonian ( $\hbar = 1$ ):  $\hat{H} = \chi\hat{J}_z^2 + \Omega_x\hat{J}_x + \Omega_y\hat{J}_y$ , where the effective interaction strength  $\chi$  and the Rabi frequencies  $\Omega_x = \text{Re}(\Omega)$  and  $\Omega_y = \text{Im}(\Omega)$  are tunable in real experiments [19, 20]. The metrology protocol starts with a Ramsey pulse ap-

plied to the BEC with all spin up, yielding a product CSS:  $|\Psi_\theta\rangle = e^{-i\theta\hat{J}_y}|J, J\rangle = |\theta, 0\rangle$ , where the polar angle  $\theta = \Omega_y t$  given by the pulse area. Next, the system evolves freely for a time  $t$ ,  $|\Psi_\theta(\phi)\rangle = e^{-i\phi\hat{J}_z}|\Psi_\theta\rangle$ , with a dimensionless phase shift  $\phi = \chi t$ . Finally, an equatorial component of the total spin  $\hat{J}_x$  or  $\hat{J}_y$  is measured to estimate  $\chi$  [13].

For nonzero  $\chi$ , the accumulated phase  $\phi$  manifests itself as oscillations of the Ramsey signal  $\langle\hat{J}_x\rangle$  or  $\langle\hat{J}_y\rangle$ , with its sensitivity quantified by [13]

$$\delta\phi_v = t\delta\chi_v = \frac{\Delta\hat{J}_v}{|d\langle\hat{J}_v\rangle/d\phi|}, \quad (v = x, \text{ or } y), \quad (1)$$

where the variance  $\Delta\hat{A} \equiv (\langle\hat{A}^2\rangle - \langle\hat{A}\rangle^2)^{1/2}$  and the expectation value  $\langle\hat{A}\rangle \equiv \langle\Psi_\theta(\phi)|\hat{A}|\Psi_\theta(\phi)\rangle$ . The  $\hat{J}_{x/y}$  measurement is achievable by applying a second  $\pi/2$  pulse after the free evolution,  $e^{-i\frac{\pi}{2}\hat{J}_{y/x}}|\Psi_\theta(\phi)\rangle$ , and following with a detection of population imbalance (i.e.,  $\hat{J}_z$ ), as done in standard Ramsey interferometry.

Collective spin excitation and external field fluctuations leads to an enhanced phase diffusion of the BEC [22]. To describe it qualitatively, we assume that free evolution of the system obeys the master equation [23, 24]:  $\dot{\rho} = i[\rho, \chi\hat{J}_z^2] + \Gamma(2\hat{J}_z\rho\hat{J}_z - \hat{J}_z^2\rho - \rho\hat{J}_z^2)$ , where  $\Gamma$  denotes the dephasing rate. For single-particle case, the second term reduces to  $\frac{\Gamma}{2}(\hat{\sigma}_z\rho\hat{\sigma}_z - \rho)$  [25]. The many-body decoherence considered here, known as the collisional dephasing [23], can be solved exactly with the density matrix element  $\rho_{m,n}(\phi) \equiv \langle J, m|\rho|J, n\rangle = \rho_{m,n}(0) \exp[i(n^2 - m^2)\phi - \gamma(m - n)^2\phi]$ , which yields

$$\langle\hat{J}_+\rangle = J e^{-\gamma\phi} \sin\theta (\cos\phi + i \cos\theta \sin\phi)^{2J-1}, \quad (2)$$

$$\langle\hat{J}_+^2\rangle = J(J-1/2) e^{-4\gamma\phi} \sin^2\theta \times (\cos 2\phi + i \cos\theta \sin 2\phi)^{2J-2}, \quad (3)$$

where  $J = N/2$ ,  $\gamma = \Gamma/\chi$ , and  $\phi = \chi t$ . Note that the collisional dephasing imposes an exponential decay to average value of  $\hat{J}_+$  and its higher moment  $\hat{J}_+^2$ , but maintains that of  $\hat{J}_z$  and  $\hat{J}_z^2$  intact, i.e.,  $\langle\hat{J}_z\rangle = J \cos\theta$  and

\*Electronic address: grjin@bjtu.edu.cn

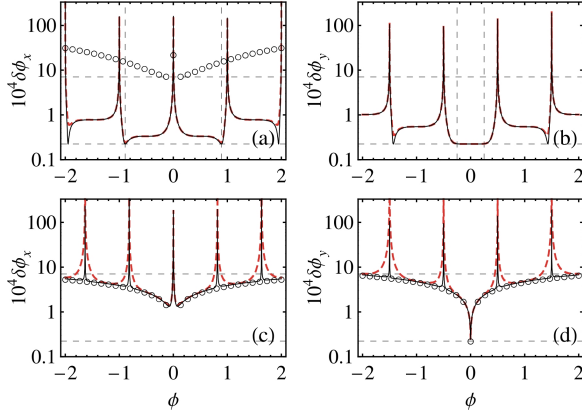


FIG. 1: (Color online) Phase sensitivities  $\delta\phi_x$  (left) and  $\delta\phi_y$  (right) as a function of phase shift  $\phi$  [in units of  $\pi/(\sqrt{2}J)$ ] for  $J = N/2 = 10^3$  and  $\gamma = 0$  (up),  $10^2$  (bottom). Solid (dashed red) lines are analytical (exact numerical) results for  $\theta = \pi/4$  (a, b, d) and  $\theta = \pi/6$  (c). Empty circles in (a) is exact result for  $\theta = \pi/2$ , while in (c) and (d) are obtained from Eq. (9) and Eq. (10) for  $\theta = \pi/6$  and  $\pi/4$ , respectively. Horizontal lines denote the Heisenberg limit  $1/(\sqrt{2}J)$  [12], and the super-Heisenberg limit  $1/(\sqrt{2}J^{3/2})$  [13]. Vertical lines in (a) and (b) correspond to  $|\phi| = 0.89\pi/(\sqrt{2}J)$  and  $0.25\pi/(\sqrt{2}J)$ , respectively.

$\langle \hat{J}_z^2 \rangle = J^2 - J(J - 1/2) \sin^2 \theta$  (c.f. Ref. [18]). The slope of the signal  $d\langle \hat{J}_{x/y} \rangle / d\phi$  corresponds to real or imaginary part of  $d\langle \hat{J}_+ \rangle / d\phi$ , with

$$\frac{d\langle \hat{J}_+ \rangle}{d\phi} = J(2J - 1)e^{-\gamma\phi}(i \cos \theta \cos \phi - \sin \phi) \times \sin(\theta)(\cos \phi + i \cos \theta \sin \phi)^{2J-2}. \quad (4)$$

We exclude the case  $\theta = 0$  and  $\pi$ , due to  $d\langle \hat{J}_v \rangle_\gamma / d\phi = 0$  and thus  $\delta\phi_v \rightarrow \infty$ , which implies no information about  $\phi$  (or  $\chi$  for a given  $t$ ) is gained from  $\hat{J}_x$  and  $\hat{J}_y$  measurements.

To obtain scaling rule of  $\delta\phi_v$ , we perform standard short-time analysis to the above exact results [17, 18]. After some straightforward calculations, we get  $(\Delta \hat{J}_x)^2 \simeq \frac{J}{2}[1 - (\eta_0 - J\eta_1) \sin^2 \theta]$ , where  $\eta_0 = \frac{1}{2}(1 + e^{-4\beta} \cos 2\alpha)$  and  $\eta_1 = (1 - e^{-2\beta})(1 - e^{-2\beta} \cos 2\alpha) + 2\phi e^{-2\beta} \cos(\theta) \sin 2\alpha$ . In the short-time limit ( $|\phi| \ll 1$ ), the parameters  $\alpha = 2J\phi \cos \theta \sim 1$  and  $\beta = J\phi^2 \sin^2 \theta + \gamma\phi \ll 1$ , which enable us to expand  $\eta_0$  ( $\eta_1$ ) up to the zeroth (the first)-order of  $\beta$ . Similarly, Eq. (4) gives  $d\langle \hat{J}_x \rangle / d\phi \simeq -J^2 \sin(\alpha) \sin 2\theta$  for  $\theta \neq \pi/2$ . As a result, we obtain

$$\delta\phi_x^2 \simeq \frac{1 + (\cos \theta \cot \alpha + 2J\phi \sin^2 \theta)^2 + 4\gamma J\phi \sin^2 \theta}{2J^3 \sin^2 2\theta}. \quad (5)$$

Replacing  $\alpha$  with  $\alpha + \pi/2$ , we also get the short-time solution of  $(\Delta \hat{J}_y)^2$  and that of the sensitivity

$$\delta\phi_y^2 \simeq \frac{1 + (\cos \theta \tan \alpha - 2J\phi \sin^2 \theta)^2 + 4\gamma J\phi \sin^2 \theta}{2J^3 \sin^2 2\theta}. \quad (6)$$

As depicted in Fig. 1, the sensitivities oscillate rapidly in a fringe pattern and diverge at  $|\phi| = s\pi/(2J \cos \theta)$  and  $(s + 1/2)\pi/(2J \cos \theta)$  for an integer  $s = 0, 1$ , etc., given by  $\cot \alpha \rightarrow \infty$  and  $\tan \alpha \rightarrow \infty$  in Eq. (5) and Eq. (6), respectively. Within central few fringes ( $s \leq 2$ ), our analytical results (thin solid lines) are coincident with the exact numerical simulations (red dashed lines).

We now analyze the achievable sensitivity for  $\hat{J}_x$  and  $\hat{J}_y$  measurements one by one. Firstly, let us consider the case  $\gamma = 0$ . Via minimizing Eq. (5) with respect to  $\phi$ , we find that local minima of  $\delta\phi_x$  occur when

$$\cos(\theta) \cot \alpha + 2J\phi \sin^2 \theta = 0, \quad \text{or} \quad \sin \alpha = \cot \theta. \quad (7)$$

The first transcendental equation gives  $(\delta\phi_x)_{\min} \simeq 1/(\sqrt{2}J^{3/2}|\sin 2\theta|)$ , as predicted in Ref. [13]. For  $\theta = \pi/4$  or  $3\pi/4$ , it becomes  $1/(\sqrt{2}J^{3/2})$ . Such a super-Heisenberg scaling of the sensitivity appears when  $\alpha = \sqrt{2}J\phi \simeq \pm 0.89\pi$ , i.e.,  $\phi_{\min} = |\chi|_{\min} t \simeq 0.89\pi/(\sqrt{2}J)$  [see Fig. 1(a)], which is valid provided  $J > 10^2$  [Fig. 2(a)]. Numerically, we also find that the best sensitivity phase  $\phi_{\min}$  depends on polar angle of the initial state  $\theta$  [empty circles of Fig. 2(b)]. For  $\pi/4 < \theta < 3\pi/4$ , it is in fact determined by  $\sin \alpha = \cot \theta$ , which predicts  $\phi_{\min} \simeq 0.2\pi/J$  for  $\theta = \pi/3$  [crosses of Fig. 2(a)].

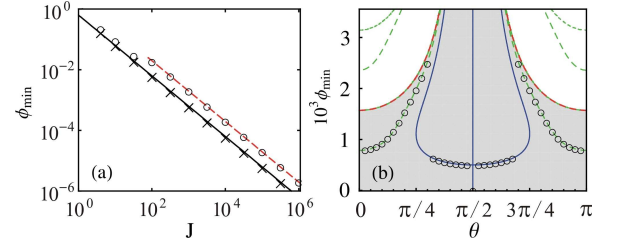


FIG. 2: (Color online) The best-sensitivity phase  $\phi_{\min}$  as a function of  $J$  (a) and  $\theta$  (b) for  $\hat{J}_x$  measurement and  $\gamma = 0$ . In (a), numerical results of  $\phi_{\min}$  for  $\theta = \pi/4$  (empty circles) and  $\pi/3$  (crosses), fit with  $0.89\pi/(\sqrt{2}J)$  (dashed red line) and  $0.2\pi/J$  (solid line). In (b), contour plots of the first (dashed green line) and the second (solid blue line) equations of (7) for  $J = 10^3$ , with numerical  $\phi_{\min}$  (empty circles). The shade region denotes the central fringe  $0 \leq \phi_{\min} < \pi/(2J \cos \theta)$ .

To proceed, we consider the  $\hat{J}_y$  measurement in the absence of the dephasing. From Eq. (6), one can find that minimal value of the sensitivity  $(\delta\phi_y)_{\min} \simeq 1/(\sqrt{2}J^{3/2}|\sin 2\theta|)$  occurs at  $\phi \sim 0$ . Obviously, the super-Heisenberg limit  $1/(\sqrt{2}J^{3/2})$  is attainable for the optimal CSS with  $\theta = \pi/4$  or  $3\pi/4$  [see Fig. 1(b), also Ref. [13]].

The above results can be casted in a more transparent form by setting  $(\delta\phi_v)_{\min} = \kappa J^{-\xi_v}$  (for  $v = x, y$ ) [13], with a pre-factor  $\kappa$  and scaling exponent

$$\xi_v = -\frac{\ln[\sqrt{2}(\delta\phi_v)_{\min}]}{\ln J} \simeq \frac{3}{2} + \frac{\ln(|\sin 2\theta|)}{\ln J}, \quad (8)$$

where we set  $\kappa = 1/\sqrt{2}$  to ensure  $\xi_v \rightarrow 3/2$  as  $\theta \rightarrow \pi/4$  or  $3\pi/4$ . One can find from Fig. 3 that without the

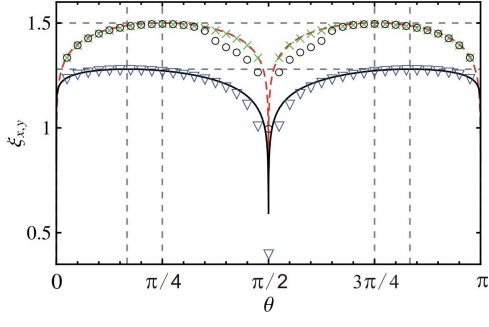


FIG. 3: (Color online) Scaling exponents  $\xi_x$  and  $\xi_y$  as a function of polar angle  $\theta$  for  $J = 10^5$ . The circles (the crosses) are numerical results of  $\xi_x$  ( $\xi_y$ ) for  $\gamma = 0$ , and the dashed red line is obtained from Eq. (8). The triangles are numerical results of  $\xi_x$  for  $\gamma = 10^3$ , and the solid line is predicted by Eq. (11). Vertical lines denote  $\theta = \pi/6, \pi/4, 3\pi/4$ , and  $5\pi/6$ ; horizontal ones correspond to  $3/2, 3/2 - \ln(2\gamma)/(3 \ln J)$ .

dephasing, numerical results of  $\xi_x$  (empty circles) and  $\xi_y$  (green crosses) agree with Eq. (8) (dashed red line).

Finally, we discuss the achievable sensitivity in the presence of the dephasing. For  $\theta \neq \pi/2$  and  $\gamma \gg 1$ , Eq. (5) and Eq. (6) can be simplified as

$$\delta\phi_x^2 \simeq \frac{1}{2J^3 \sin^2 2\theta} [(4J\phi)^{-2} + 4\gamma J\phi \sin^2 \theta], \quad (9)$$

$$\delta\phi_y^2 \simeq \frac{1}{2J^3 \sin^2 2\theta} [1 + 4\gamma J\phi \sin^2 \theta], \quad (10)$$

which correspond to the envelope curves of the sensitivities [see empty circles of Figs. 1(c) and (d)]. For  $\hat{J}_x$  measurement, the best sensitivity  $(\delta\phi_x)_{\min}^2 \simeq 3\gamma^{2/3}/(8J^3 \sin^{2/3} \theta \cos^2 \theta)$ , and thus

$$\xi_x \simeq \frac{3}{2} + \frac{\ln(\frac{2}{\sqrt{3}}\gamma^{-1/3} \sin^{1/3} \theta |\cos \theta|)}{\ln J}. \quad (11)$$

As shown in Fig. 3, our analytical result shows a good agreement with numerical simulations (triangles) for the dephasing rate  $1 \ll \gamma < J^{3/4}$ . Remarkably, the optimal scaling  $\xi_x \simeq 3/2 - \ln(2\gamma)/(3 \ln J)$  is obtained at  $\theta = \pi/6$  or  $5\pi/6$ , which leads to the best-sensitivity phase  $\phi_{\min} \simeq 1/[J(2\gamma)^{1/3}]$  with  $(\delta\phi_x)_{\min} \simeq (2\gamma)^{1/3}/(\sqrt{2}J^{3/2})$ . For  $\hat{J}_y$  measurement, the phase  $|\phi| \sim s\pi/(\sqrt{2}J)$  (with an integer  $s \leq 2$ ) can be detected at the super-Heisenberg limit provided  $\theta = \pi/4$  or  $3\pi/4$ . However, the sensitivity for  $|\phi| > 2\pi/(\sqrt{2}J)$  degrades rapidly [see Fig. 1(d)].

In summary, we have derived analytical results for pre-estimation of effective interaction strength  $\chi$  in a two-component BEC. Without collisional dephasing, the best-sensitivity phase  $\phi_{\min}$  for  $\hat{J}_x$  measurement depends on the initial CSS  $|\theta, 0\rangle$  and bifurcates at  $\theta \sim \pi/4$  or  $3\pi/4$  (see Fig. 2b). In the presence of the dephasing (with  $1 \leq \gamma < J^{3/4}$ ), the optimal CSS becomes  $|\theta = \pi/6, 0\rangle$ , and the achievable sensitivity is reduced by a factor of  $(2\gamma)^{1/3}$  below the scaling  $1/(\sqrt{2}J^{3/2})$ . Our analytical results confirm that the detection of  $\hat{J}_y$ , i.e., the  $\hat{J}_z$  measurement to the output state  $e^{-i\frac{\pi}{2}\hat{J}_x}e^{-i\phi\hat{J}_z^2}e^{-i\frac{\pi}{4}\hat{J}_y}|J, J\rangle$ , shows its advantages since phase estimation of  $\phi \sim 0$  can reach the super-Heisenberg limit even in the presence of the dephasing [13].

This work is supported by the NSFC (Contract No. 10804007) and the SRFDP (Contract No. 200800041003). L.Y. is partially supported by the NKBRF of China under Grants 2006CB921206 and 2006AA06Z104.

- 
- [1] C. M. Caves, Phys. Rev. D **23**, 1693 (1981).
  - [2] B. Yurke, S. L. McCall, and J. R. Klauder, Phys. Rev. A **33**, 4033 (1986).
  - [3] M. J. Holland and K. Burnett, Phys. Rev. Lett. **71**, 1355 (1993).
  - [4] D. J. Wineland, J. J. Bollinger, W. M. Itano, and D. J. Heinzen, Phys. Rev. A **50**, 67 (1994).
  - [5] D. Leibfried, M. D. Barrett, T. Schaetz, *et al.*, Science **304**, 1476 (2004).
  - [6] M. W. Mitchell, J. S. Lundeen, and A. M. Steinberg, Nature **429**, 161 (2004).
  - [7] V. Giovannetti, S. Lloyd, and L. Maccone, Science **306**, 1330 (2004); *ibid*, Phys. Rev. Lett. **96**, 010401 (2006).
  - [8] J. J. Bollinger, W. M. Itano, D. J. Wineland, and D. J. Heinzen, Phys. Rev. A **54**, R4649 (1996).
  - [9] R. A. Campos, C. C. Gerry, and A. Benmoussa, Phys. Rev. A **68**, 023810 (2003).
  - [10] P. M. Anisimov, G. M. Raterman, A. Chiruvelli, *et al.*, Phys. Rev. Lett. **104**, 103602 (2010).
  - [11] A. Luis, Phys. Lett. A **329**, (2004).
  - [12] A. M. Rey, L. Jiang, and M. D. Lukin, Phys. Rev. A **76**, 053617 (2007).
  - [13] S. Boixo, A. Datta, S. T. Flammia, *et al.*, Phys. Rev. A **77**, 012317 (2008).
  - [14] S. Choi and B. Sundaram, Phys. Rev. A **77**, 053613 (2008).
  - [15] M. J. Woolley, G. J. Milburn, and C. M. Caves, New J. Phys. **10**, 125018 (2008).
  - [16] A. Sørensen, L.-M. Duan, J. I. Cirac, and P. Zoller, Nature **409**, 63 (2001).
  - [17] M. Kitagawa and M. Ueda, Phys. Rev. A **47**, 5138 (1993).
  - [18] G. R. Jin, Y. C. Liu, and W. M. Liu, New J. Phys. **11**, 073049 (2009); G. R. Jin, B. B. Wang, and Y. W. Lu, Chinese Phys. B **19**, 020502 (2010).
  - [19] C. Gross, T. Zibold, E. Nicklas, *et al.*, Nature **464**, 1165 (2010).

- [20] M. F. Riedel, P. Böhi, Y. Li, *et al.*, Nature **464**, 1170 (2010).
- [21] A. Widera, O. Mandel, M. Greiner, *et al.*, Phys. Rev. Lett. **92**, 160406 (2004).
- [22] A. Widera, S. Trotzky, P. Cheinet, *et al.*, Phys. Rev. Lett. **100**, 140401 (2008).
- [23] R. R. Puri and G. S. Agarwal, Phys. Rev. A **45**, 5073 (1992); T. W. Chen and P. T. Leung, Phys. Rev. A **67**, 055802 (2003).
- [24] Y. Khodorkovsky, G. Kurizki, and A. Vardi, Phys. Rev. A **80**, 023609 (2009).
- [25] S. F. Huelga, C. Macchiavello, T. Pellizzari, *et al.*, Phys. Rev. Lett. **79**, 3865 (1997).